JOURNAL OF AIRCRAFT
Vol. 31, No. 3, May–June 1994

Unsteady Blade Pressures on a Propfan: Predicted and Measured Compressibility Effects

M. Nallasamy*
Sverdrup Technology, Inc., Brook Park, Ohio 44142

The effect of compressibility on unsteady blade pressures is studied by solving the three-dimensional Euler equations. The operation of the eight-bladed SR7L propfan at 4.75-deg angle of attack was considered. Euler solutions were obtained for three Mach numbers, 0.6, 0.7, and 0.8, and the predicted blade pressure waveforms were compared with flight data. The predictions show that the change in pressure waveforms are minimal when the Mach number is increased from 0.6 to 0.7, as observed in the flight experiments. Increasing the Mach number from 0.7 to 0.8 produces significant changes in predicted pressure levels. The predicted amplitudes, however, differ from measurements at some transducer locations. Also, the predicted appearance of a shock in the highly loaded portion of the blade revolution is not indicated by the measurements. At all three Mach numbers the measured (installed propfan) pressure waveforms at the majority of transducer locations show a relative phase lag compared to the computed (propfan alone) waveforms. This appears to be due to installation effects. Measured waveforms in the blade tip region show nonlinear variations which are not captured by the present numerical procedure.

Introduction

THE flow unsteadiness affects critically the propfan performance and near-field noise levels. The unsteadiness may be the result of operation of the propfan at an angle relative to the mean flow direction, or of distorted inflow caused by installation effects. Wind-tunnel and flight tests were conducted on a 2.74-m- (9-ft-) diam large-scale propfan to further understand the effects of flow unsteadiness.[1–3]

Unsteady blade pressure measurements of the large-scale propfan were first made in a transonic wind tunnel with angular inflow and (cylinder) wake inflow.[1] It was found that at takeoff conditions, high-power cases resulted in the formation of a leading-edge vortex on the blade. Then, in the propfan test assessment (PTA) program, flight tests were conducted to investigate the effect of inflow angle on the near-field noise level.[2] A sensitivity of about 1 dB per degree of inflow angle change was found in flight measurements. Finally, in the PTA follow-on flight tests, detailed unsteady blade pressure measurements[3] were made on a specially designed instrumented blade. In this test, the blade suction surface had 20 pressure transducers distributed over three radial stations (r/R = 0.68, 0.86, and 0.95, where r is the radial distance and R is the blade tip radius), while the pressure surface had 10 pressure transducers distributed over two radial stations (r/R = 0.68 and 0.95). A nacelle tilt arrangement was employed to vary the inflow angle to the propfan.

Three sets of data were taken providing a unique data base of detailed unsteady blade pressures in flight: 1) low altitude (580 m), low speed (Mach number ~0.3); 2) high altitude (10,500 m), high speed (Mach number ~0.8); and 3) a compressibility series in which the flight Mach number M was varied (Mach number ~0.6, 0.7, and 0.8), keeping the advance ratio and power coefficient (blade angle) constant. In each set, three nacelle tilt angles, −3, −1 (tilt down), and 2 deg (tilt up), were considered, giving an effective inflow angle variation of 5 deg. Efforts have been made to understand the unsteady flow features exhibited by these data and also to validate the prediction of three-dimensional Euler analysis methods against the data.

The unsteady flow features of a propfan at takeoff (low speed, low altitude) were examined by Nallasamy[4] by solving the three-dimensional Euler equations. It was found that the measured (installed propfan) blade pressure waveforms showed a relative phase lag compared to the computed (propfan alone) waveforms at the outboard (r/R = 0.95) station on both pressure and suction surfaces. However, on the pressure surface the magnitudes were found to be in good agreement with flight data at all inflow angles studied. On the suction surface, in addition to the relative phase lag, the measurements showed distortion of the waveforms. The extent of distortion increased with inflow angle.

Nallasamy and Groeneweg[5] studied the unsteady flow features at cruise operating conditions. They showed that at inflow angles of 1.6 and 4.6 deg, passage shocks extending from suction to pressure surface formed and dissolved during each revolution of the blade. The computed unsteady blade pressures for 1.6 deg were compared with wind-tunnel data.[6] The comparisons showed good agreement of the predicted blade pressure waveforms with data at most of the transducer locations considered.

The effect of compressibility on steady blade pressures was examined.[7] It was found that with increasing Mach number, more significant changes occurred on the suction side than on the pressure side. The evidence of a compression wave started to develop when the Mach number reached 0.7. At a free-stream Mach number of 0.78, the compression wave fully developed into a trailing-edge shock.

In this article, the effects of compressibility on unsteady blade pressures of a propfan are studied by solving the three-dimensional Euler equations for angular inflow. The solutions are obtained for three Mach numbers, 0.6, 0.7, and 0.8 of the PTA follow-on compressibility test series, keeping advance ratio and blade angle constant. First, the predicted blade pressure waveforms for M = 0.8 are compared directly with PTA follow-on flight data to assess the predictions at the high inflow angle, high-speed case. Then the waveforms for three Mach numbers, 0.6, 0.7, and 0.8, are compared with measured waveforms to evaluate the ability of the solution procedure in predicting the Mach number effects observed in

Presented as Paper 92-3774 at the AIAA/SAE/ASME/ASEE 28th Joint Propulsion Conference, Nashville, TN, July 6–8, 1992; received July 19, 1992; revision received Jan. 26, 1993; accepted for publication April 23, 1993.

*Acting Deputy Director, Aeromechanics Department, NASA Lewis Research Center Group. Member AIAA.

flight tests. No effort is made here to quantify the effect of compressibility on propfan performance.

Numerical Solution of Three-Dimensional Euler Equations

The unsteady three-dimensional Euler equations governing the inviscid flow through a propfan are solved employing a solution procedure developed by Whitfield et al.[8,9] In this procedure the Euler equations in conservative differential form are transformed from a Cartesian reference frame to a body-fitted curvilinear reference frame. The transformed equations are then discretized employing a finite volume technique. A lower-upper (LU) implicit numerical scheme is used to solve the discretized equations. An approximate Riemann solver is used for block interface definitions. The flowfield is represented by a multiblock composite grid to limit the core memory requirements.

Flow Configuration and Computational Grid

The configuration considered is that of the eight-bladed SR7L propfan of the flight test.[3] The direction of rotation of the propfan is clockwise, looking downstream. The azimuth angle Φ is measured from vertical (top-dead-center) for aircraft installation as in the presentation of flight data in Ref. 3, and increases in the direction of rotation (Fig. 1). The grid employed is an H-grid with 107 × 41 × 25 (axial by radial by circumferential) nodal points in each passage. The blade design hot coordinates are used to generate the grid. Each passage is divided into three blocks with 107 × 41 × 9 grid points in each block. Thus, 24 blocks of grid were used to describe the entire flowfield. Each blade surface is represented by 49 × 27 (axial by radial) grid points with higher resolution near the leading and trailing edges, the hub and the tip.

Table 1 PTA follow-on test cases[3]: predicted and measured total power coefficients

Run no.	Mach no.	Blade angle		Power coefficient	
		Test	Euler	Test	Euler
140	0.8	56.7	57.0	1.493	1.491
142	0.7	56.6	57.0	1.533	1.549
144	0.6	55.5	57.0	1.475	1.386

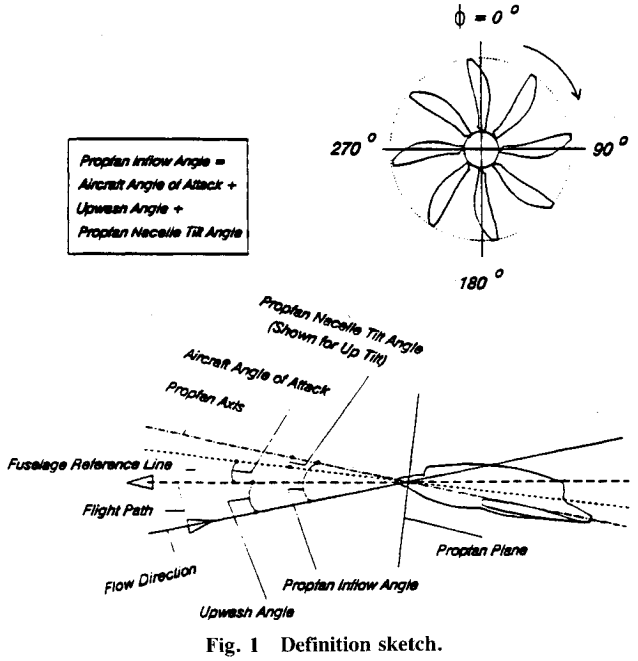

Fig. 1 Definition sketch.

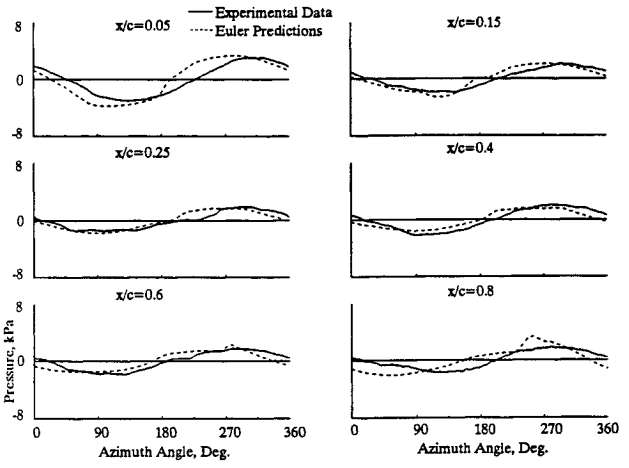

Fig. 2 Pressure waveforms on the suction surface at r/R = 0.68, M = 0.8.

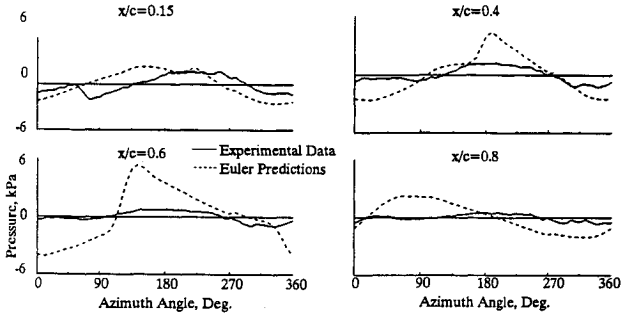

Fig. 3 Pressure waveforms on the pressure surface at r/R = 0.68, M = 0.8.

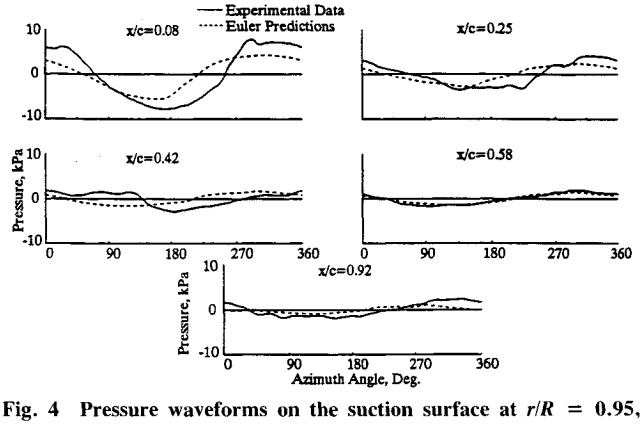

Fig. 4 Pressure waveforms on the suction surface at r/R = 0.95, M = 0.8.

Results and Discussion

The unsteady three-dimensional Euler solutions were obtained for the following three flight test cases of Ref. 3: 1) run = 144, i.d. = 1 c and M = 0.603; 2) run = 142, i.d. = 2 c, M = 0.701; and 3) run = 140, i.d. = 3 c and M = 0.803. These three runs had a nacelle tilt of +2 deg. The effective inflow angle is dependent not only on the nacelle tilt angle but also on the airplane angle of attack and the upwash angle at the propfan (Fig. 1). For the above test runs, the average value of the airplane angle of attack was 1.75 deg. The estimated upwash[5] at the propfan was 1.0 deg. Therefore, the effective inflow angle to the propfan was 4.75 deg. The Euler solutions were obtained with an advance ratio of 3.17, blade setting angle of 57 deg, and inflow angle of 4.75 deg for all three Mach numbers.

The Euler solutions are obtained from an impulse start for three complete revolutions of the blade, to obtain a reason-

ably accurate solution. The results of the third revolution are analyzed and presented here. The predicted total power coefficient (for eight blades) are shown in Table 1 along with the measured ones. In the experiments, the blade angle for $M = 0.6$ is different from the other two. In the predictions, though the blade angle (57 deg) is maintained the same for all Mach numbers, the total power coefficient is under-predicted by about 6% for $M = 0.6$. The total power coefficients for $M = 0.7$ and 0.8 are in reasonable agreement with data. In all three cases, the power per blade variation was found to show the expected sinusoidal variation due to inflow angle. The amplitude of the stabilized power coefficient during the third revolution varies +109% and −98% about the mean for $M = 0.6$, +120%, and −102% for $M = 0.7$ and +105% and −104% for $M = 0.8$.

First, the predicted and measured blade pressure waveforms are compared for the high Mach number case, $M = 0.8$. Figure 2 shows the blade pressure waveforms at the transducer locations (x/c, where x is the axial distance and c is the blade chord) on the suction surface at the inboard radial station $r/R = 0.68$. The predicted amplitudes agree fairly well with flight data. The measured waveforms show a relative phase lag compared to the predicted ones. This is in contrast to the takeoff case studied,[4] where such a phase lag was observed only at the outboard radial station. The observed phase lag seems to be due to installation effect, i.e., the presence of the wing in flight tests as compared to the propfan alone configuration of the computation. Heidelberg and Woodward[10] noted similar phase variations in their model tests in the wind tunnel with and without wing installation. In the present flight tests, the measured waveforms show a relative phase lag that varies from 17 to 47 deg. The minimum lag, 17 deg, occurs at $x/c = 0.4$, whereas near the leading edge, $x/c = 0.05$, the lag is about 37 deg, and near the trailing edge, $x/c = 0.8$, it is 47 deg. It should be noted that the comparison of waveforms predicted using the same solution technique with the propfan alone, wind-tunnel measured waveforms did not show any such phase lags.[6,11]

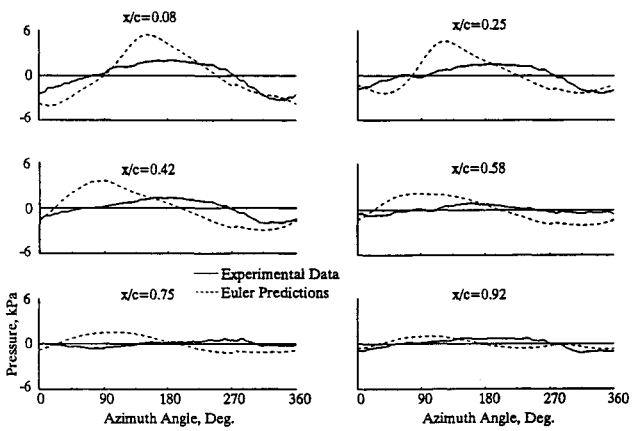

Fig. 5 Pressure waveforms on the pressure surface at $r/R = 0.95$, $M = 0.8$.

In Ref. 5 detailed flowfield information in blade passages were presented in the form of instantaneous static pressure contours at one spanwise station, $r/R = 0.66$ (Fig. 7 in Ref. 5). For an inflow angle of 4.6 deg, significant flow changes were found to occur in blade passages. A shock formed in the trailing-edge region of suction surface in the highly loaded part of the revolution extends across the passage to the pressure side of the successive blade. No shock formation is observed on the lightly loaded part of the revolution.

In the present case, for $M = 0.8$ and inflow angle of 4.75 deg, similar flowfield features are observed. That is, the numerical solution produces a passage shock during the highly loaded part of the revolution (see Fig. 6 and the associated discussion below). This results in the predicted blade pressure waveform on the pressure surface, shown in Fig. 3. The measurements do not show such a shock formation. The measured blade response is quite small at transducer locations $x/c = 0.6$ and 0.8. At the transducer locations $x/c = 0.15$ and 0.4, the waveform is somewhat distorted from the sinusoidal form, the reasons for which are not known. Thus, the present predictions present an altogether different picture from the measured one. Also, the measured waveforms at $x/c = 0.15$ and 0.8 show a phase lag compared to the predictions, whereas

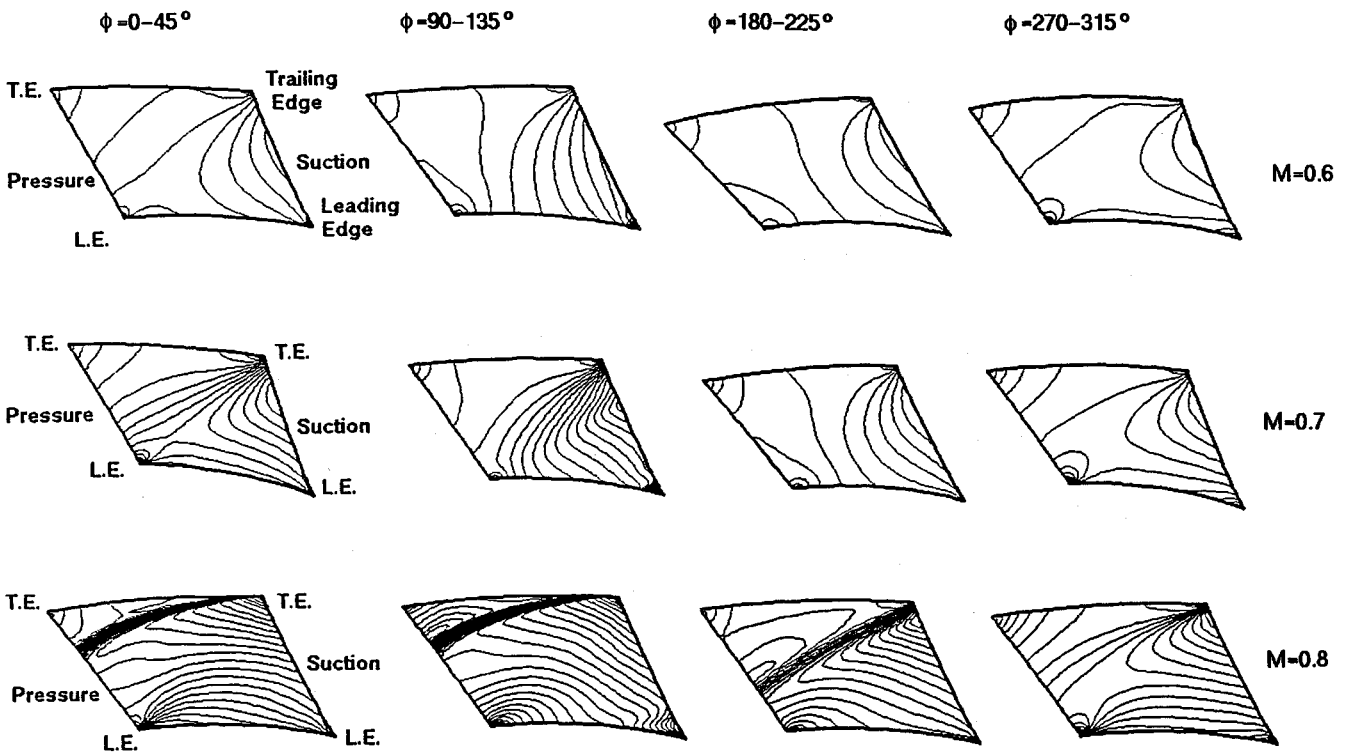

Fig. 6 Instantaneous static pressure contours in the blade passages at $r/R = 0.68$ (min = 0.352; max = 1.017; contour interval = 0.0133).

at $x/c = 0.4$ and 0.6, a phase lead is observed. A more detailed study is needed to establish if the appearance of a passage shock is real and not an artifact of the numerical scheme employed. However, another Euler solution scheme employed by Hall et al.[12] also show such passage shock formation at a similar inflow angle and Mach number. Figure 4 shows the blade pressure waveforms at the transducer locations on the suction surface at the outboard radial station, $r/R = 0.95$. Near the leading edge, the peak amplitude is underpredicted. The relative phase lag of the measured waveform compared to the computed ones exist at all transducer locations, except that at $x/c = 0.58$, and it is in the range of 34–47 deg. At $x/c = 0.58$, the measured waveform shows a small relative phase lead compared to the predictions.

The blade pressure waveforms on the pressure surface at the outboard radial station are shown in Fig. 5. The passage shock, discussed above with reference to Fig. 3, extends until the tip region. This causes the predicted blade pressure waveforms to be quite different from the measurements since no shock is observed at any radial station. Figure 5 shows blade pressure waveforms at the outboard radial station, $r/R = 0.95$. At these transducer locations, the magnitudes are substantially overpredicted. Also, significant differences in shape of the waveforms are observed. However, a waveform of shape similar to that predicted at $x/c = 0.25$ has been observed in wind-tunnel tests,[6] on the pressure surface for an inflow angle of 2 deg (e.g., see Fig. 5c in Ref. 6). However, it has not been possible to establish clearly if the differences between the predicted and measured waveforms stem from the installation effect or not, due to lack of similar wind-tunnel data at the high inflow angle considered here. At this outboard radial station, $r/R = 0.95$, the value of relative phase lag of the measured waveform also varies widely. At $x/c = 0.75$ and 0.92, the blade response is low and the predicted waveform is nearly 180 deg out of phase with that of flight measurement. This appears to be due to the strong interaction of the blade wake and tip vortex flows, and it is not clear as to the kind of interaction that would produce such a phase variation.

Compressibility effects: detailed flowfield information in the form of static pressure contours in the blade passages is shown in Fig. 6 for the three Mach numbers, 0.6, 0.7, and 0.8, at the radial station, $r/R = 0.68$. Figure 6 shows the pressure contours only in four (alternate) blade passages, 0–45, 90–135, 180–225, and 270–315 deg. Each picture in Fig. 6 shows the static pressure contours in the radial plane ($r/R = 0.68$) bounded by the suction surface of a blade on one side (e.g., $\Phi = 45$ deg), the pressure surface of the successive blade (e.g., $\Phi = 0$ deg) on the opposite side, the (grid) line connecting the leading edges (L.E.) of the two blades, and the (grid) line connecting the trailing edges (T.E.). At Mach 0.8, a shock formed in the trailing-edge region of the suction surface, in the highly loaded part of the revolution, extends across the passage to the pressure side of the successive blade. No shock is observed in the lightly loaded part of the revolution or at low Mach numbers. It should be noted that the present computations do not include the viscous effects. Including viscous effects may influence the location and strength of the shock. As mentioned above, Hall et al.[12] have also observed such passage shocks at $M = 0.8$, with their Euler analysis technique.

The effect of Mach number on unsteady blade pressure is demonstrated in Figs. 7 and 8, in terms of blade surface pressure contours. The blade surfaces shown are the same surfaces of successive blades that define blade passages in Fig. 6. Figure 7 shows the blade pressure at four azimuthal positions ($\Phi = 45$, 135, 225, and 315 deg) on the suction surface for all three Mach numbers. The blade pressure variation during a revolution is clearly seen to be significant at each Mach number—for the high inflow angle—4.75 deg, considered here. The range of pressure variation during a revolution is, of course, maximum for $M = 0.8$. Of particular interest is $\Phi = 135$-deg position (in the highly loaded part of the revolution), where the area of low pressure region increases with increase in Mach number. Figure 8 shows the blade pressures at four azimuthal positions ($\Phi = 0$, 90, 180, and 270 deg) on the pressure surface for three Mach numbers. It is seen that the

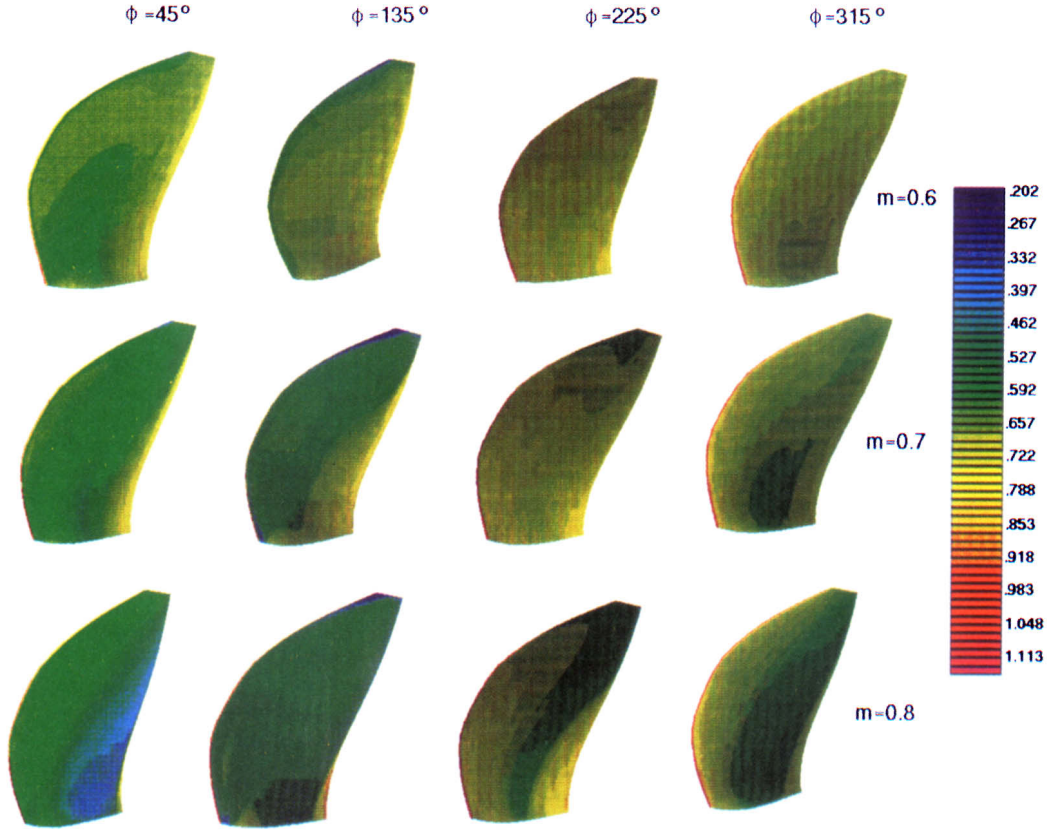

Fig. 7 Instantaneous blade pressure distribution on the suction surface.

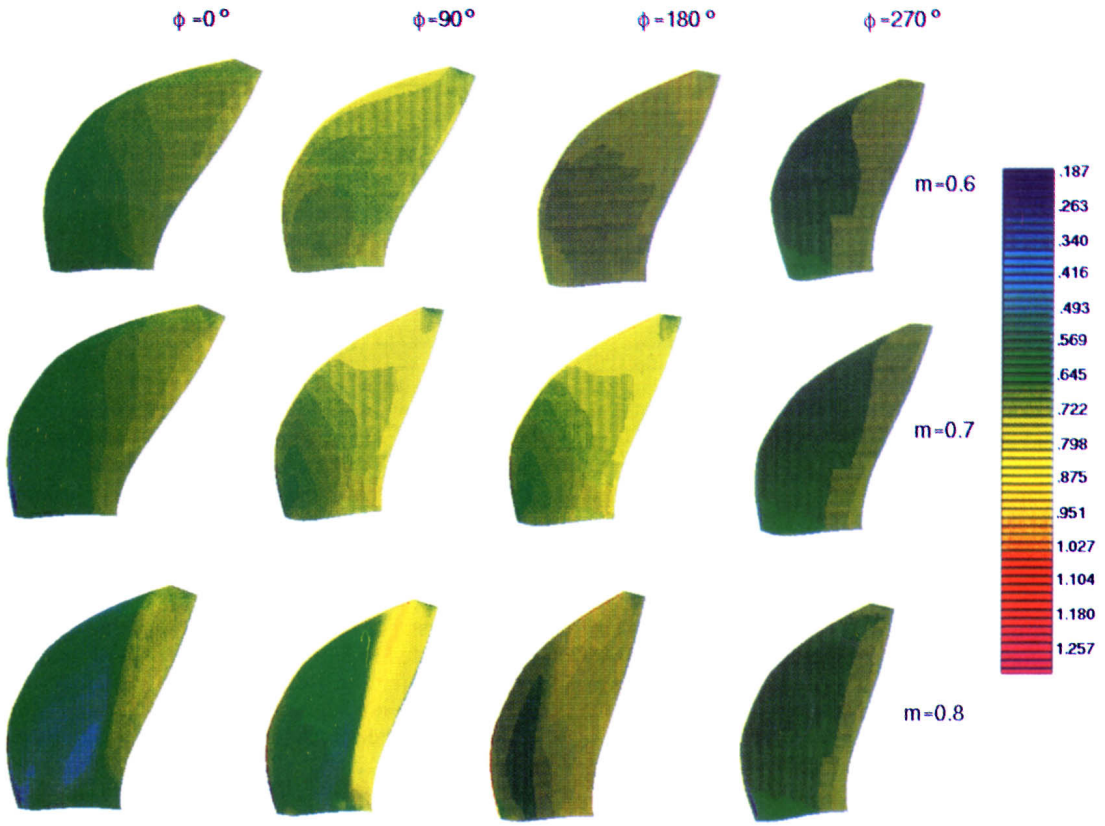

Fig. 8 Instantaneous blade pressure distribution on the pressure surface.

cyclic variation of the blade pressure during a revolution is nearly the same for Mach numbers 0.6 and 0.7. But at $M = 0.8$, a shock appears (in the highly loaded region) at $\Phi = 90$ deg. The shock shows maximum strength at this location, which also corresponds to a strong passage shock in the blade passage, $\Phi = 90$–135 deg in Fig. 6. The experimental data, however, do not indicate such a shock formation.

Next, we present the predicted blade pressure waveform variations with Mach number along with the flight data. For clarity, the predicted and measured data are presented side by side to show the compressibility effect in each case in all the succeeding figures. Figure 9 shows the predicted and measured waveforms at the transducer locations on the suction surface at $r/R = 0.68$. First of all, it is observed that the measured waveforms show a relative phase lag compared to the predicted ones at all the three Mach numbers. In general, the effect of increasing Mach number on the waveform is well predicted. Exceptions occur near the leading edge, $x/c = 0.05$, where the maximum amplitudes are overpredicted for $M = 0.6$ and 0.7. The predictions tend to produce a higher blade response near the leading edge at all Mach numbers except $M = 0.8$. The measurements in most cases, however, show a blade response near the leading edge which is much smaller than the maximum response at that radial station. The difference appears to be due to viscous effects which are not considered here. Boundary layer on the blade and transition to turbulence may contribute to these differences. The kinks in the waveforms at the transducer locations $x/c = 0.6$ and 0.8 indicates the presence of a passage shock which extends from near the trailing edge of the suction surface to the pressure surface of the successive blade (Fig. 6).

The predicted and measured waveforms on the pressure surface at $r/R = 0.68$ are shown in Fig. 10 for three Mach numbers. As in most predictions, the Euler solution shows that the blade response is highest near the leading edge. The same is shown here, and in this case the measurements also show similar behavior. However, due to the appearence of a predicted shock in the passage for $M = 0.8$, the waveforms are in disagreement with the measurements. The plots show that when the Mach number is increased from 0.6 to 0.7, very little change occurs in the waveforms, both in prediction and experiments. However, the magnitudes are overpredicted. For $M = 0.8$, the predicted waveforms show sharp changes in magnitudes indicative of the presence of a shock (as shown in Fig. 8). But the experimental waveforms show that only near the leading edge, $x/c = 0.15$, a noticeable change in waveform occurs when the Mach number is increased to 0.8. The relative phase lag of the measured waveforms persists at all Mach numbers.

For the outboard radial station, $r/R = 0.95$, a comparison of predicted and measured waveforms is presented in Fig. 11. First, it is observed that the measured waveforms are distorted from sinusoidal form at most of the transducer locations at all Mach numbers. The predictions show that at each Mach number, the largest response occurs near the trailing edge, except for $M = 0.7$, for which the transducer at $x/c = 0.92$ has a higher response than the one ahead. The measurements, however, indicate that the maximum response occurs at $x/c = 0.42$. The measured waveform is distorted from the linear sinusoidal form of the predicted one. The waveform distortion may occur due to viscous effects manifested in the form of a separation bubble as suggested by the low pressure (within the bubble) at $\Phi \sim 160$ deg (peak loading) and steep rise in pressure outside the bubble. Since viscous effects are not considered here, the broadening or the steepening of the waveform are not captured in the present predictions. The magnitudes are underpredicted. However, one trend is correctly predicted, i.e., with an increase in Mach number, the response decreases at $x/c = 0.25$ and 0.42.

Euler solutions are known to predict qualitatively the formation of tip vortex[13] in steady (zero angle of attack) flow. For angular inflow, the measurements seem to indicate that the spatial extent of the tip vortex on the blade (suction surface) depends on azimuthal position. During a highly loaded part of the revolution, the tip vortex may extend over the transducer at $x/c = 0.08$, 0.25, 0.42, and 0.58. An adaptive

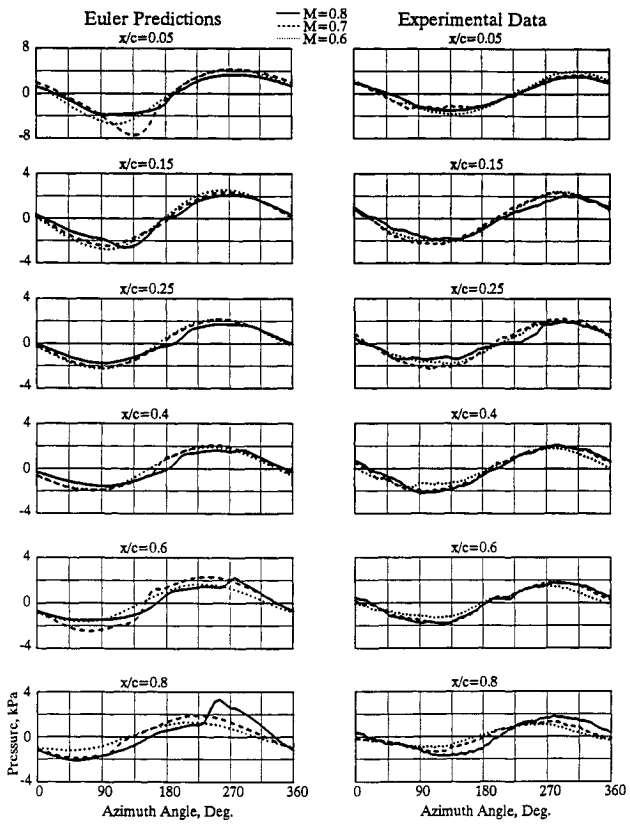

Fig. 9 Predicted and measured pressure waveforms on the suction surface at $r/R = 0.68$.

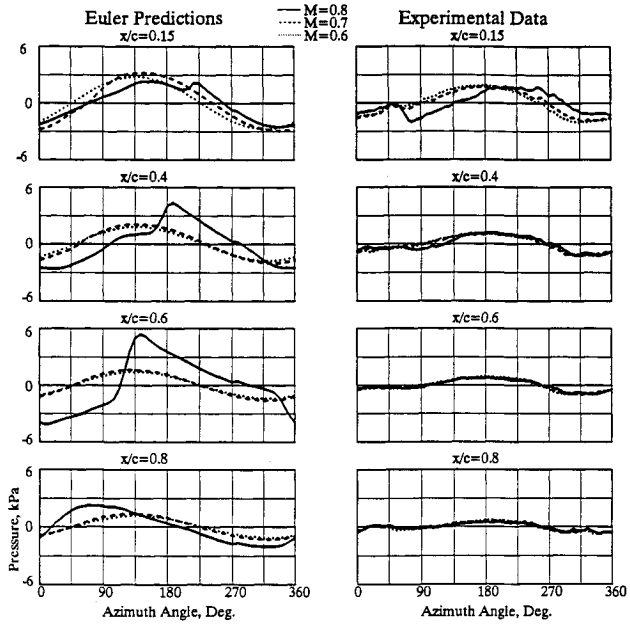

Fig. 10 Predicted and measured pressure waveforms on the pressure surface at $r/R = 0.68$.

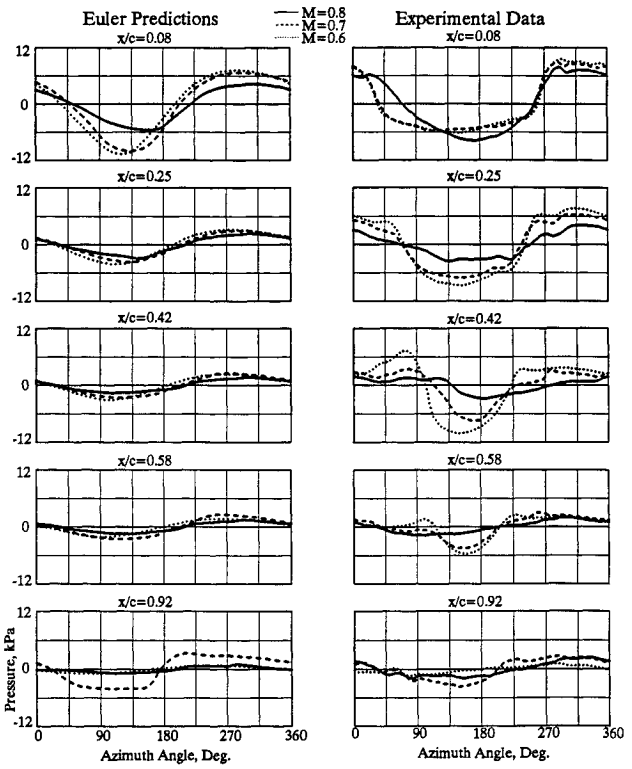

Fig. 11 Predicted and measured pressure waveforms on the suction surface at $r/R = 0.95$.

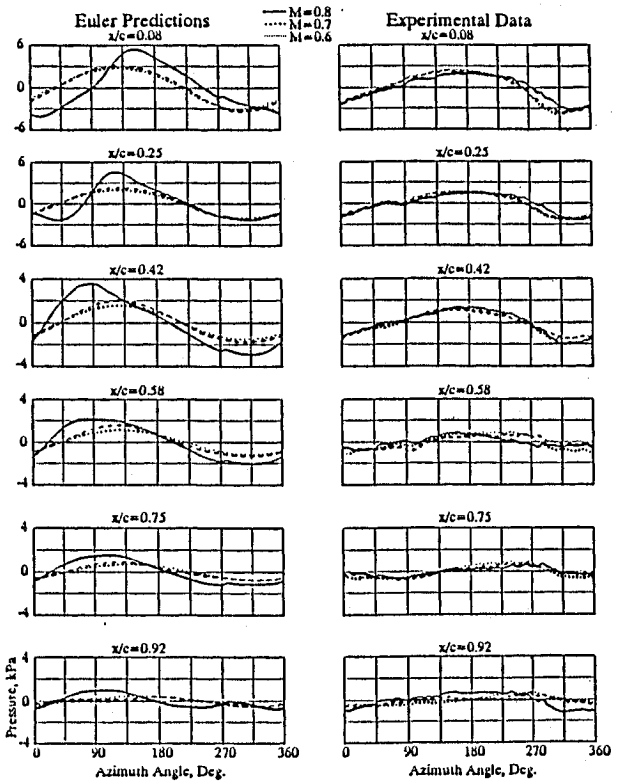

Fig. 12 Predicted and measured pressure waveforms on the pressure surface at $r/R = 0.95$.

grid which can correctly track the extent of the tip vortex and its strength at all azimuthal positions, may be able to improve the predictions in the outboard region.

Figure 12 shows the pressure waveforms on the pressure surface at the outboard radial station, $r/R = 0.95$. The measured waveforms are relatively insensitive to Mach number at this radial station, at all transducer locations. The predicted waveforms show little change when the Mach number is increased from 0.6 to 0.7. But when the Mach number is increased to 0.8, due to the appearance of a passage shock as mentioned earlier, the predicted waveforms differ in shape and magnitude. In general, at all Mach numbers, the maximum response occurs near the leading edge, and the response reduces gradually towards the trailing edge, both in measurement and prediction. Significant relative phase lag of the measured waveform is observed at all transducer locations compared to the predicted ones.

Concluding Remarks

The effect of compressibility on unsteady blade pressures was studied by solving the three-dimensional Euler equations. The unsteadiness is due to the operation of the propfan at 4.75-deg angle of attack. Three Mach numbers, 0.6, 0.7, and 0.8 were considered, and the predicted waveforms were compared with flight data.

Comparison of predicted and measured waveforms shows the following: the changes in pressure waveforms are minimal when the Mach number is increased from 0.6 to 0.7 (except on the suction surface at $r/R = 0.95$); and increasing the Mach number from 0.7 to 0.8 produces significant differences in predicted pressure levels. The predicted appearance of a shock at this Mach number is not indicated by the experiments. The measured waveforms show a relative phase lag compared to the predicted ones at the majority of the transducer locations. The phase lag appears to be due to the installation effect, i.e., the installed propfan of the flight test compared to the propfan alone configuration of the computation. In the present study, the blade design hot coordinates were used for the grid generation. No dynamic blade shape due to unsteady loading was calculated. It is not clear if part of the observed phase lag arises from the unsteady blade deflection.

The present numerical procedure is unable to reproduce the nonlinear variations of the measured waveforms. On the suction surface (near the tip region) the measured waveforms also show distortion (widening and steepening) which decreases with increase in Mach number. This distortion appears to be due to viscous effects. Consideration of the viscous effects, and perhaps an adaptive grid technique which accurately captures the extent and strength of the tip vortex, may improve the predictions in the outboard region. The present numerical technique as well as others (e.g., Ref. 12) show the existence of a shock at $M = 0.8$, whereas the measurements do not. A more detailed experimental and numerical study is needed to resolve this inconsistency.

Acknowledgment

This work is sponsored by NASA Lewis Research Center under Contract NAS3-25266 with John F. Groeneweg as Project Manager.

References

[1]Bushnell, P., Gruber, M., and Parzych, D., "Measurement of Unsteady Blade Surface Pressures on a Single-Rotation Large-Scale Advanced Propfan with Angular and Wake Inflow at Mach Numbers from 0.02 to 0.70," NASA-CR-182123, Oct. 1988.

[2]Little, B. H., Bartel, H. W., Reddy, N. N., Swift, G., Withers, C. C., and Brown, P. C., "Propfan Test Assessment (PTA) Flight Test Report," NASA-CR-182278, July 1989.

[3]Parzych, D., Boyed, L., Mesissner, W., and Wyrostek, A., "In Flight Measurement of Steady and Unsteady Blade Surface Pressure of a Single Rotation Large-Scale Advanced Propfan Installed on the PTA Aircraft," NASA-CR-187096, Sept. 1991.

[4]Nallasamy, M., "Unsteady Blade Pressures on a Propfan at Takeoff: Euler Analysis and Flight Data," AIAA Paper 92-0376, Jan. 1992.

[5]Nallasamy, M., and Groeneweg, J. F., "Unsteady Euler Analysis of the Flowfield of a Propfan at an Angle of Attack," *Journal of Propulsion and Power*, Vol. 8, No. 1, 1992, pp. 136–143.

[6]Heidelberg, L. J., and Nallasamy, M., "Unsteady Blade Pressures Measurements for the SR-7A Propeller at Cruise Conditions," AIAA Paper 90-4022, Oct. 1990.

[7]Nallasamy, M., Yamamoto, O., Wasrsi, S., and Bober, L. J., "Large-Scale Advanced Propeller Blade Pressure Distributions: Prediction and Data," *Journal of Propulsion and Power*, Vol. 7, No. 3, 1991, pp. 452–461.

[8]Whitfield, D. L., Swafford, I. W., Janus, J. M., Mulac, R. A., and Belk, D. M., "Three-Dimensional Unsteady Euler Solutions for Propfans and Counter-Rotating Propfans," AIAA Paper 87-1197, June 1987.

[9]Janus, J. M., and Whitfield, D. L., "A Simple Time Accurate Turbomachinery Algorithm with Numerical Solutions of Uneven Blade Count Configuration," AIAA Paper 89-0206, Jan. 1989.

[10]Heidelberg, L. J., and Woodward, R. P., "Advanced Turboprop Wing Installation Effects Measured by Unsteady Blade Pressure and Noise," AIAA Paper 87-2719; see also NASA-TM-100200, Oct. 1987.

[11]Nallasamy, M., and Groeneweg, J. F., "Unsteady Blade Surface Pressures on a Large-Scale Advanced Propeller: Prediction and Data," *Journal of Propulsion and Power*, Vol. 7, No. 6, 1991, pp. 866–872.

[12]Hall, E. J., Delaney, R. A., and Bettner, J. L., "Investigation of Advanced Counter-Rotation Blade Configuration Concepts for High Speed Turboprop Systems, Task II Unsteady Ducted Propfan Analysis," NASA-CR-187106, May 1991.

[13]Nallasamy, M., Clark, B. J., and Groeneweg, J. F., "Euler Analysis of the Three-Dimensional Flow Field of a High-Speed Propeller: Boundary Condition Effects," *Journal of Turbomachinery*, Vol. 109, 1987, pp. 332–339.